Quantum Creep in $Y_{1-x}Pr_xBa_2Cu_3O_{7-\delta}$ Crystals: Magnetic Relaxation and Transport

T. Stein, G. A. Levin, and C. C. Almasan
Department of Physics, Kent State University, Kent, Ohio 44242

D. A. Gajewski and M. B. Maple
Department of Physics and Institute for Pure and Applied Physical Sciences, University of California, San Diego, La Jolla, California 92093

(Received 30 December 1998)

We report transport and magnetic relaxation measurements in the mixed state of strongly underdoped $Y_{1-x}Pr_xBa_2Cu_3O_{7-\delta}$ crystals. A transition from thermally activated flux creep to temperature-independent quantum flux creep is observed in both transport and magnetic relaxation at temperatures $T \leq 5$ K. Flux transformer measurements indicate that the crossover to quantum creep is preceded by a coupling transition. Based on these observations we argue that below the coupling transition the current is confined within a very narrow layer beneath the current contacts. [S0031-9007(99)08855-9]

PACS numbers: 74.60.Ge, 74.50.+r, 74.72.Bk

Quantum flux creep in superconductors is the only experimentally accessible phenomenon in which a macroscopic metastable system, such as a persistent supercurrent, relaxes coherently without thermal activation. In all other metastable systems, the relaxation proceeds as a sequence of a large number of uncorrelated microscopic steps, requiring thermal activation over an energy barrier. Yet, the evidence of magnetic relaxation and resistance that do not extrapolate to zero at a temperature $T \rightarrow 0$ has not reached a point where experimental data begin to form a cohesive picture of the phenomenon. While the nonvanishing magnetic relaxation has been observed both in single crystals and thin films [1–3], the nonvanishing temperature-independent resistance had been observed only in ultrathin films and multilayers [4–6]. This has contributed to the assertion that the temperature-independent resistance in films and the nonvanishing low-temperature magnetic relaxation in single crystals are unrelated phenomena.

A second question, closely related to quantum creep in high-T_c superconductors, is the coupling transition in layered crystals. Several groups have arrived at conflicting conclusions. Safar *et al.* [7] reported that the voltages generated by the motion of vortices on the opposite faces of the $YBa_2Cu_3O_{7-\delta}$ sample (flux transformer method) converge. However, such a strong manifestation of the coupling transition appears to be the exception rather than the rule. Other groups have observed that the voltages generated on the opposite faces of $Bi_2Sr_2CaCu_2O_8$ [8–11] and $YBa_2Cu_3O_{7-\delta}$ [12] crystals diverge with lowering temperature, rather than converge.

Here we report the results of both magnetic relaxation and transport measurements on strongly underdoped crystals of $Y_{0.47}Pr_{0.53}Ba_2Cu_3O_{7-\delta}$ ($T_c \approx 17$–21 K). Our transport data indicate that the onset of quantum creep is preceded by a coupling transition which leads to non-Ohmic dissipation. The transition to temperature-independent creep takes place at lower T and only in a very thin layer below the current contacts; the rest of the sample continues to exhibit thermally activated creep. A picture of the low-temperature dissipation of the transport current that arises from these observations is that the sample is divided into two macroscopic regions: a very thin layer, a few unit cells thick, near the upper face, where the current contacts are located, which carries most of the current, and the rest of the sample which remains mostly undisturbed by the current. These two macroscopic regions are decoupled from each other. Inside these layers the vortices are coherent, with the correlation length comparable to the thickness of the respective layer. Magnetic relaxation measurements confirm the transition to T-independent relaxation at approximately the same temperatures as in transport.

Two strongly underdoped twinned single crystals of $Y_{0.47}Pr_{0.53}Ba_2Cu_3O_{7-\delta}$ with $T_c \approx 17$ and 21 K, respectively, were prepared as described in Ref. [13]. The first sample was used for transport measurements with the "flux transformer" contact configuration [inset to Fig. 1(a)]: The current I was injected through the contacts on one face of the sample and the voltage drop between the voltage contacts on the same (primary voltage V_p) and the opposite (secondary voltage V_s) faces was measured for temperature, total current, and magnetic field H, applied parallel to the c axis, in the ranges $1.9 \leq T \leq 25$ K, $0.3\ \mu\text{A} \leq I \leq 2$ mA, and $0.2 \leq H \leq 9$ T. Magnetic relaxation measurements were performed on the second crystal using a SQUID magnetometer. The crystal was cooled in zero field; a field $H + \Delta H$ ($\Delta H = 0.3$ T for all H) was applied parallel to its c axis, and then the field was reduced to H. The decay of the resultant paramagnetic moment was monitored for several hours ($\approx 10^4$ s).

Figure 1(a) gives an overview of the T and H dependence of V_p and V_s normalized to I and H. The convergence of these curves at $T \approx 9$ K indicates a regime of free flow of vortices, where $V_{p,s}/I \propto H$. In a region

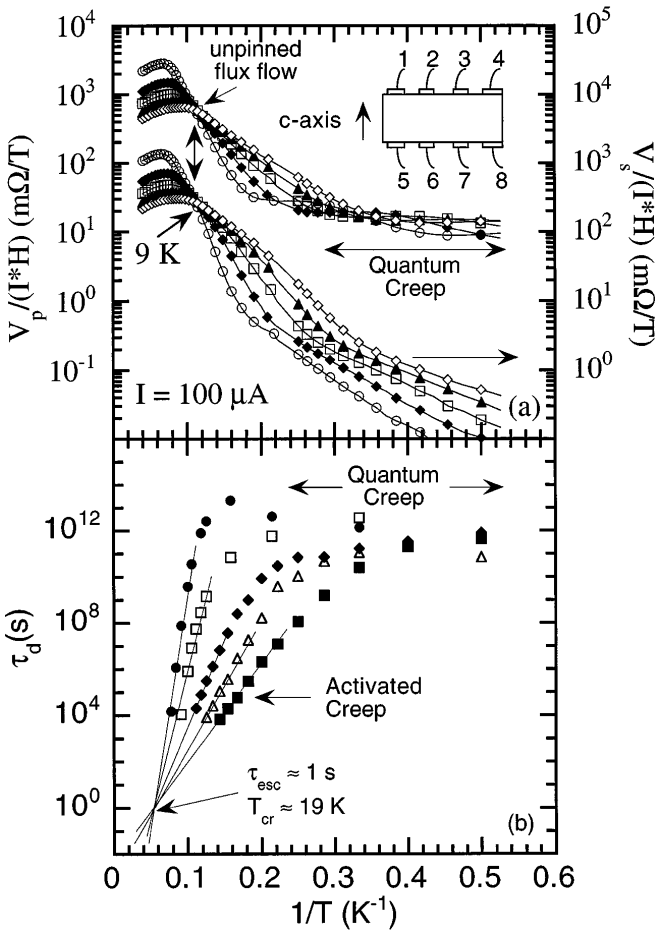

FIG. 1. (a) Primary V_p and secondary V_s voltages, normalized to the total current I and magnetic field H, plotted vs $1/T$ for five magnetic fields (0.2, 0.4, 0.6, 0.8, and 1 T). The slope decreases with increasing field. Inset: Contact configuration used in the measurements. (b) Decay time τ_d of magnetic moment (see definition in text) vs $1/T$ for $H = 0.1$, 0.2, 0.6, 0.8, and 1.2 T. The slope decreases with increasing field. The straight line extrapolations of the Arrhenius-type dependence converge at $T_{cr} \approx 18-19$ K and $\tau_{esc} \approx 1-2$ s. The saturation of τ_d at the level $10^{11}-10^{12}$ s is due to quantum creep.

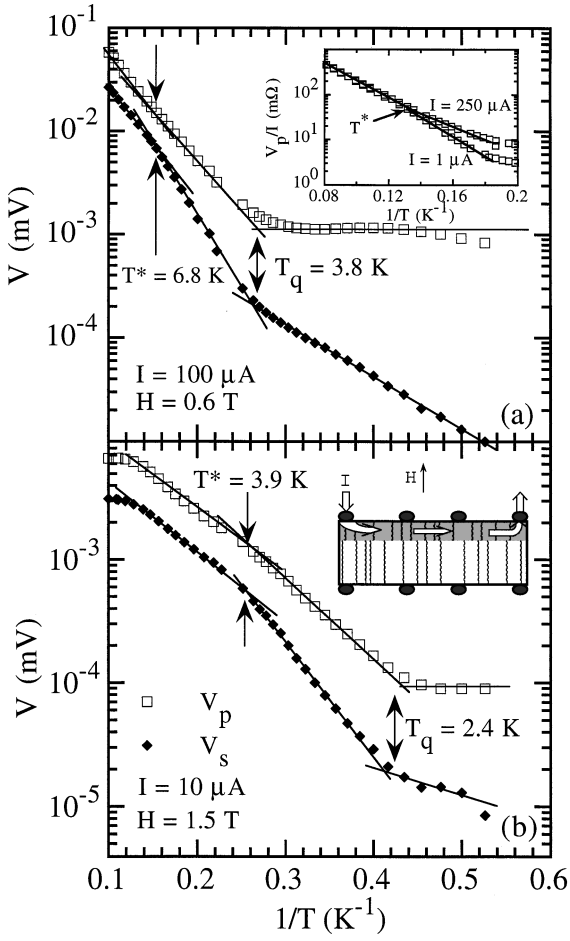

FIG. 2. Arrhenius plots of the primary V_p and secondary V_s voltages measured in two different fields and currents: (a) $H = 0.6$ T and $I = 100$ μA, and (b) $H = 1.5$ T and $I = 10$ μA. Inset to (a): Expanded view of the primary resistance V_p/I for two values of the total current (1 and 250 μA) in an applied magnetic field $H = 0.2$ T. Inset to (b): Schematic representation of the current distribution. The current flows mainly in the upper (shaded) layer. The vortices are coupled within each layer, but the layers are decoupled from each other.

below 9 K, V_p and V_s exhibit activated T dependences with field-dependent activation energies. At even lower T, the primary signal becomes T independent and scales approximately with H, while the secondary voltage remains thermally activated.

Figures 2(a) and 2(b) represent an expanded view of $V_{p,s}$ vs $1/T$ for $H = 0.6$ T, $I = 100$ μA and $H = 1.5$ T, $I = 10$ μA, respectively. The activation energies $E_{p,s} \equiv -d \ln V_{p,s}/d(1/T)$ of both V_p and V_s suddenly change at a temperature $T^*(H)$. In addition, the dissipation becomes strongly non-Ohmic below T^*. As the inset to Fig. 2(a) shows, the primary resistance $R_p(T) \equiv V_p/I$ is current independent only above T^*. The activation energies $E_{p,s}$, which are equal and current independent at $T > T^*$, become current dependent at $T < T^*$. At low current, the activation energy below T^* is *greater* than above T^* [Fig. 2(b)] so that the curves $V_{p,s}(1/T)$ have a downward curvature. However, the activation energy decreases with increasing current and $E_p(I)$ becomes smaller than it is at $T > T^*$, so that $V_p(1/T)$ acquires an upward curvature [V_p in Fig. 2(a) and the inset].

This evidence indicates that the vortices undergo a coupling transition at T^*. At $T > T^*$, the dissipation mechanism is activated hopping of 2D pancakes over potential barriers since the activation energies are the same for the primary and secondary voltages, in spite of the nonuniform current distribution. When the pancakes begin to form coherent lines, the activation energy increases so that $V_{p,s}(1/T)$ curve downward. However, the fact that V_p remains greater than V_s (below T^*, V_p/V_s rapidly increases with decreasing T) indicates that the vortices do not extend through the whole sample.

An important fact for understanding the nature of dissipation below T^* is that the activation energy decreases with increasing current and eventually becomes *smaller* than that for 2D pancakes. Figure 3 displays the current

dependence of $U_p^{3D} \equiv E_p$ at $T < T^*$ for $H = 0.2$ T. The double arrow indicates the value of the current independent $U^{2D} \equiv E_{p,s}$ at $T > T^*$ and for the same magnetic field. The fact that $U_p^{3D} < U^{2D}$ for $I > 0.2$ mA indicates that the vortices remain coupled even at large currents which allows a new channel of relaxation to emerge and become dominant due to smaller activation energy. The inset to Fig. 3 is a log-log plot of U_s^{3D} vs H, obtained from the secondary voltage V_s (limit of very small current). The values of U_s^{3D} follow an $H^{-1/2}$ dependence. This field dependence of U_s^{3D} is consistent with a 3D plastic creep model, where U_s^{3D} is estimated as the energy needed for the formation of a double kink over the Peierls barrier [14,15]. These results show that the dissipation at $T < T^*$ is determined by two parallel processes: Thermally activated motion of correlated vortices (dominant at low currents) with the activation energy greater than that for 2D pancake vortices and plastic motion of dislocations (dominant at higher currents) with the activation energy smaller than that for a 2D vortex.

At lower temperatures, the primary voltage V_p becomes temperature independent for $T < T_q(H)$ and scales approximately with the field [Fig. 1(a)] while V_s remains thermally activated, but with a noticeably smaller activation energy (Fig. 2).

The high normal state resistivity of this specimen may be the reason that quantum creep begins to dominate the thermally activated process at relatively high temperatures $T_q \sim 5$ K. A previous study has shown that the normal state resistivity $\rho_n(T)$ of this crystal (revealed by the suppression of superconductivity with a large magnetic field) is insulating, similar to that of $PrBa_2Cu_3O_{7-\delta}$, so

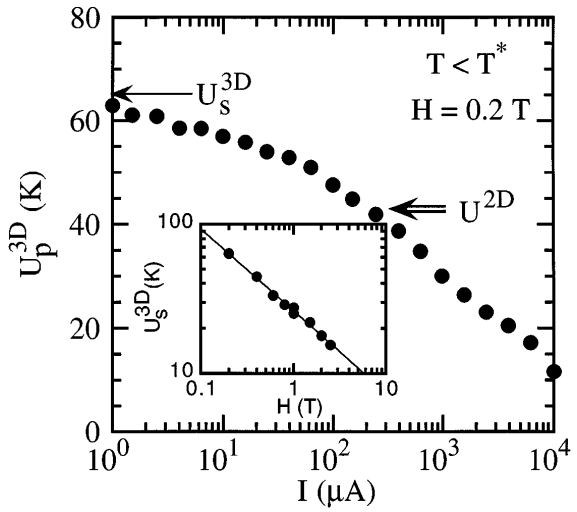

FIG. 3. Current dependence of the activation energy U_p^{3D} determined as $d \ln V_p / d \ln(1/T)$ for $T < T^*$ in a field $H = 0.2$ T. In the limit of small current, $U_p^{3D} \approx U_s^{3D}$ as shown by the arrow. The value of $U^{2D} \approx 45$ K is also indicated by the double arrow. Inset: Field dependence of the activation energy U_s^{3D} determined as $d \ln V_s / d \ln(1/T)$ for $T < T^*$. The solid line corresponds to $H^{-1/2}$ dependence.

that $\rho_n(T) \rightarrow \infty$ at $T \rightarrow 0$ [16]. The reduced dissipation in the normal core of a vortex due to a large normal-state resistivity increases the mobility of the vortices and facilitates tunneling [14].

The succession of the coupling transition by quantum creep points towards the model of flux flow shown schematically in the inset to Fig. 2(b). Below T^* the vortices begin to form coherent lines and the dissipation becomes non-Ohmic. The transport current is mostly confined within a narrow layer below the current contacts. The rest of the sample remains relatively undisturbed. These two regions of the sample are uncoupled and, inside each of them, the vortices are coherent over a distance comparable to the thickness of the respective layer. In this scenario, the large resistive anisotropy in the mixed state results from the loss of the phase coherence only between two macroscopic regions of the sample, not between all microscopic layers (such as CuO_2 bilayers) as in the 2D phase at $T > T^*$. The fact that at $T < T_q$ we observe a T-independent V_p and a thermally activated V_s indicates that the thickness of the current-carrying layer is just a few unit cells (which makes it similar to ultrathin films and multilayers, the only other systems in which quantum creep was observed in transport measurements). The small length of vortices makes tunneling a dominant mechanism even at relatively high temperatures ($T \approx 5$ K); the vortices in the lower layer (which is the bulk of the sample) do not tunnel because of the much longer correlation length and, therefore, V_s remains activated.

This scenario raises the possibility that the transport current undergoes self-channeling at $T < T^*$. At temperatures *above* T^*, the $Y_{1-x}Pr_xBa_2Cu_3O_{7-\delta}$ crystals are not very anisotropic; for the crystal studied (length $L \approx 1$ mm and thickness $D \approx 0.015$ mm), the ratio $V_p/V_s \sim 2$ at $T > T^*$, so that the transport current fills the cross section fairly uniformly. On the other hand, the transition to quantum creep, which is extremely sensitive to the length of the tunneling segments, indicates that near T_q, the current-carrying volume collapses into a layer just a few unit cells thick. A possible reason may be the nonlinear relationship between the current density and electric field in the mixed state below T^*. The nonlinear resistive anisotropy may result in instability of the current distribution with respect to formation of a very thin current-carrying channel.

In order to confirm that the T-independent V_p [Fig. 1(a)] is the result of quantum flux creep, we performed magnetic relaxation measurements on a similar crystal. At higher temperatures the relaxation of the magnetic moment proceeds as a sequence of uncorrelated microscopic steps, each involving thermal activation over a certain energy barrier U. The decay time τ_d during which the induced moment loses a *substantial fraction* of its initial value can be defined as

$$\tau_d = \tau_{\rm esc} \exp\left\{\frac{U(H,T)}{T}\right\}, \qquad (1)$$

where the Boltzmann factor reflects the degree of availability of energy U required for an average elementary step and is essentially independent of the physics of the relaxation process, while the preexponential factor $\tau_{\rm esc}$ is a measure of how rapidly the relaxation would proceed, had it not been limited by unavailability of thermal energy. We call $\tau_{\rm esc}$ the *escape time,* to distinguish it from the microscopic attempt time τ_a which characterizes the period of vibration of the vortex inside a pinning well. The escape time may depend on the sample size, magnetic field, and temperature. Factorization of τ_d given by Eq. (1) is meaningful as long as the Boltzmann factor $\exp(U/T) \gg 1$, so that it dominates the T and H dependence of τ_d. With $U(H,T) = U_0(H)\,(1 - T/T_{\rm cr})$, where $T_{\rm cr}$ is the temperature at which the activation energy vanishes, the decay time becomes

$$\tau_d = \tau_{\rm esc} \exp\left\{U_0(H)\left(\frac{1}{T} - \frac{1}{T_{\rm cr}}\right)\right\}. \qquad (2)$$

We emphasize that Eq. (1) is more general than any particular dynamic model of the relaxation process driven by fluctuations.

Within the decade of time 10^3–10^4 s, the magnetic relaxation curves are well fitted to $M_{irr} = a - b\ln(t/t_0)$, where t_0 is an arbitrary unit of time. Because of the slowness of the relaxation, the decay time cannot be determined directly by monitoring the induced moment until it loses a substantial fraction of its initial value. An alternative method, which we will use, is to estimate the decay time by extrapolating the $M_{irr}(t)$ dependence to $M_{irr}(\tau_d) = 0$, which gives

$$\tau_d = t_0 \exp\{a/b\}. \qquad (3)$$

With this definition, τ_d is universal and does not depend on the choice of t_0 so that we can compare the experimental τ_d with Eq. (2). Figure 1(b) shows τ_d calculated according to Eq. (3) and plotted vs $1/T$ for different values of H. At higher temperatures the data display an Arrhenius dependence with a slope $d\ln\tau_d/d(1/T)$ decreasing with increasing H. The trend is consistent with the field dependence of the activation energy in transport measurements, Fig. 1(a).

According to Eq. (2), the preexponential factor $\tau_{\rm esc}$ can be determined by the extrapolation of the Arrhenius dependence of $\tau_d(T)$ to $T = T_{\rm cr}$. Indeed, the straight lines extrapolating the activated dependence converge at $T_{\rm cr} \approx 19$ K $\approx T_c$ and $\tau_d = \tau_{\rm esc} \approx 1$ s. The value of $\tau_{\rm esc}$ is consistent with the time it takes for a vortex to diffuse from the bulk to the outer edge of the sample: $\tau_{\rm esc} \sim R^2/\mathcal{D}_v \sim R^2/\omega_a\ell_a^2$, where R is the characteristic size of the sample in the direction of diffusion, and $\mathcal{D}_v$ is the diffusion coefficient determined by the attempt frequency ω_a and the average hopping distance ℓ_a. With $\tau_{\rm esc} \sim 1$ s and $R^2 \sim 10^{-2}$–10^{-3} cm^2 (for the crystal we used), $\mathcal{D}_v \sim 10^{-2}$–$10^{-3}$ cm^2/s. This value of $\mathcal{D}_v$ is consistent with an elementary step of the order of the correlation length $\ell_a \sim 100$ Å and $\omega_a \sim 10^{11}$–10^{12} s^{-1}.

At lower temperatures, the decay time saturates at a roughly T- and H-independent level [Fig. 1(b)]. The values of $T_q(H)$ from transport [(Fig. 1(a)] and magnetic relaxation [Fig. 1(b)] measurements are very close in spite of a very large difference in the currents involved in these measurements. The fact that the transition to a temperature-independent dissipation takes place in both transport and magnetic relaxation processes, and at approximately the same temperature in a given field indicates that both phenomena have the same origin. The Euclidean action S_E can be estimated as $S_E/\hbar = \ln(\tau_d/\tau_{\rm esc}) \approx 25$, which is comparable, but somewhat smaller than previously reported values for other systems [3].

This research was supported at KSU by the National Science Foundation under Grants No. DMR-9601839 and No. DMR-9801990, and at UCSD by U.S. Department of Energy under Grant No. DE-FG03-86ER-45230.

[1] A. C. Mota, G. Juri, P. Visani, A. Pollini, T. Teruzzi, and K. Aupke, Physica (Amsterdam) **185C–189C**, 343 (1991).
[2] A. J. J. van Dalen, R. Griessen, S. Libbrecht, Y. Bruynseraede, and E. Osquiguil, Phys. Rev. B **54**, 1366 (1996).
[3] A. F. Th. Hoekstra, R. Griessen, A. M. Testa, J. el Fattahi, M. Brinkmann, K. Westerholt, W. K. Kwok, and G. W. Crabtree, Phys. Rev. Lett. **80**, 4293 (1998).
[4] Y. Liu, D. B. Haviland, L. I. Glazman, and A. M. Goldman, Phys. Rev. Lett. **68**, 2224 (1992).
[5] D. Ephron, A. Yazdani, A. Kapitulnik, and M. R. Beasley, Phys. Rev. Lett. **76**, 1529 (1996).
[6] J. A. Chervenak and J. M. Valles, Jr., Phys. Rev. B **54**, R15 649 (1996).
[7] H. Safar, P. L. Gammel, D. A. Huse, S. N. Majumdar, L. F. Schneemeyer, D. J. Bishop, D. Lopez, G. Nieva, and F. de la Cruz, Phys. Rev. Lett. **72**, 1272 (1994).
[8] R. Busch, G. Ries, H. Werthner, G. Kreiselmeyer, and G. Saemann-Ischecnko, Phys. Rev. Lett. **69**, 522 (1992).
[9] H. Safar, E. Rodriguez, F. de la Cruz, P. L. Gammel, L. F. Schneemeyer, and D. J. Bishop, Phys. Rev. B **46**, 14 238 (1992).
[10] R. A. Doyle, W. S. Seow, Y. Yan, A. M. Campbell, T. Mochiku, K. Kadowaki, and G. Wirth, Phys. Rev. Lett. **77**, 1155 (1996).
[11] C. D. Keener, M. L. Trawick, S. M. Ammirata, S. E. Hebboul, and J. C. Garland, Phys. Rev. B **55**, R708 (1997).
[12] Y. Eltsev, W. Holm, and O. Rapp, Phys. Rev. B **49**, 12 333 (1994).
[13] L. M. Paulius, B. W. Lee, M. B. Maple, and P. K. Tsai, Physica (Amsterdam) **230C**, 255 (1994).
[14] G. Blatter, M. V. Feigel'man, V. B. Geshkenbein, A. I. Larkin, and V. M. Vinokur, Rev. Mod. Phys. **66**, 1125 (1994).
[15] Y. Abulafia, A. Shaulov, Y. Wolfus, R. Prozorov, L. Burlachkov, Y. Yeshurun, D. Majer, E. Zeldov, H. Wuhl, V. B. Geshkenbein, and V. M. Vinokur, Phys. Rev. Lett. **77**, 1596 (1996).
[16] G. A. Levin, T. Stein, C. C. Almasan, S. H. Han, D. A. Gajewski, and M. B. Maple, Phys. Rev. Lett. **80**, 841 (1998).